and C6/7. Bar=1cm for A-C, 50μm for D.

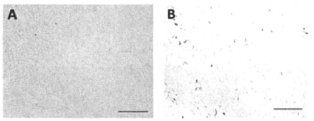

Figure 4

GFAP staining shows the glial reaction is comparatively rare around the cystic cavity. Low magnification (A) and high magnification (B). Bar= 50μm for A, 20μm for B.

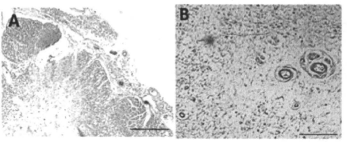

Figure 5

Elastica van Gieson (EVG) staining of vessels adjacent to the cystic cavity. Low magnification view shows vessels are distributed around cystic cavity (A). Magnification view of A shows these vessels have a thickened outer membrane with hyaline degeneration (B). Bar= 50μm for A, 20μm for B.

JOURNAL OF NEUROTRAUMA 27:2283–2294 (December 2010)

DOI: 10.1089/neu.2009.1144

Interferon-γ Decreases Chondroitin Sulfate Proteoglycan Expression and Enhances Hindlimb Function after Spinal Cord Injury in Mice

Takayuki Fujiyoshi,[1,2] Takekazu Kubo,[1] Carmen C.M. Chan,[1] Masao Koda,[2] Akihiko Okawa,[2] Kazuhisa Takahashi,[2] and Masashi Yamazaki[2]

Abstract

Glial cells, including astrocytes and macrophages/microglia, are thought to modulate pathological states following spinal cord injury (SCI). In the present study, we evaluated the therapeutic effects of interferon-γ (IFN-γ), which is one of the cytokines regulating glial function, in a mouse contusive SCI model. We found that intraperitoneal injection of IFN-γ significantly facilitated locomotor improvement following SCI. Immunohistochemistry demonstrated that IFN-γ decreased the accumulation of chondroitin sulfate proteoglycans (CSPGs), which are critical axon outgrowth inhibitors produced by reactive astrocytes in the injured central nervous system (CNS). Quantitative real-time polymerase chain reaction (RT-PCR) and Western blotting demonstrated that neurocan, one of several CSPGs, was reduced in the spinal cords of IFN-γ-treated mice compared to vehicle-treated mice. Consistently, IFN-γ inhibited the production of neurocan from activated astrocytes *in vitro*. In addition, IFN-γ treatment enhanced the number of serotonin-positive nerve fibers and myelinated nerve fibers around the lesion epicenter. We also found that glial cell line-derived neurotrophic factor (GDNF) and insulin-like growth factor-1 (IGF-1) were upregulated post-SCI following IFN-γ treatment. Our results indicate that IFN-γ exhibits therapeutic effects in mouse contusive SCI, presumably by reducing CSPG expression from reactive astrocytes and increasing the expression of neurotrophic factors.

Key words: astrocyte; interferon-γ; chondroitin sulfate proteoglycan; macrophage; microglia; neurotrophic factors; spinal cord injury

Introduction

INJURED AXONS in the central nervous system (CNS) regenerate poorly compared to those of the peripheral nervous system (PNS). Subsequent to spinal cord injury (SCI), the lack of axonal regeneration results in permanent functional deficits. Traumatic injury of the spinal cord causes the recruitment of glial cells including astrocytes and macrophages/microglia to the injured site, and these glial cells play positive and negative roles in axonal regeneration and functional recovery post-SCI (Donnelly and Popovich, 2008; Popovich and Longbrake, 2008; Yiu and He, 2006). Reactive astrocytes at the injured site are detrimental to axonal regeneration post-SCI, since they form a glial scar that constitutes a physical barrier to axon regeneration. They also produce chondroitin sulfate proteoglycans (CSPGs), that are potent axon outgrowth inhibitors (McKeon et al., 1991, 1999; Smith and Strunz, 2005; Yiu and He, 2006). It has been suggested that the blockade of the inhibitory effects of CSPGs is of potential therapeutic value in the treatment of SCI. Intrathecal infusion of chondroitinase ABC, which is a bacterial enzyme that cleaves glycosaminoglycan side chains on CSPGs, into the injured spinal cord has been demonstrated to overcome the inhibitory effect of CSPGs, and results in axon regrowth and functional recovery in rodents (Barritt et al., 2006; Bradbury et al., 2002).

Macrophages/microglia are also reported to play roles in the pathogenesis of CNS injuries. The beneficial effects of macrophages/microglia include the clearance of axon and myelin debris by phagocytic action/protease secretion, and the promotion of axon elongation/neuronal survival by the secretion of neurotrophic factors (Donnelly and Popovich, 2008; Jones et al., 2005; Popovich and Longbrake, 2008; Schwartz et al., 1999; Shechter et al., 2009). However, it has been suggested that the activation of macrophages/microglia after CNS injury is less efficient than that of macrophages after

Departments of [1]Neurobiology and [2]Orthopaedic Surgery, Graduate School of Medicine, Chiba University, Chiba, Japan.

PNS injury, and that this might be partly attributable to the deficiency of appropriate regeneration of the injured CNS (Schwartz et al., 1999). It is of interest that the implantation of activated macrophages promotes axonal growth and functional recovery following CNS injury (Lazarov-Spiegler et al., 1996; Rapalino et al., 1998). Conversely, the excessive inflammation associated with tissue injuries mainly induced by macrophages/microglia can also be detrimental to recovery post-SCI (Donnelly and Popovich, 2008; Jones et al., 2005; Popovich and Longbrake, 2008). Inflammatory cytokines such as tumor necrosis factor-α (TNF-α) and/or interleukin-1 (IL-1) expressed by activated macrophages/microglia induce neurodegeneration following SCI (Genovese et al., 2006; Lee et al., 2000; Nesic et al., 2001). A recent report showed that inflammation itself is required for spinal cord repair (Stirling et al., 2009). Thus anti-inflammatory cytokines do not always promote recovery after SCI, and appropriate doses of proinflammatory cytokines might be helpful for the SCI repair process.

In this study, we demonstrate that a proinflammatory cytokine, interferon-γ (IFN-γ), which modulates the activities of both astrocytes and macrophages/microglia and is clinically available for the treatment of mycosis fungoides in humans, has therapeutic effects on an experimental mouse contusion model of SCI.

Methods

The mouse animal model of spinal cord injury

Adult female C57BL/6 mice (8–10 weeks old) were anesthetized with 1–1.2% halothane in oxygen. Following dorsal laminectomy (T9–T10 level), the spinal cord was contused (60 kdyn) using an Infinite Horizon Impactor (Precision Systems & Instrumentation, West Monroe, LA), as previously described (Koda et al., 2007; Nishio et al., 2007). The muscle and skin layers were then sutured. The bladder was expressed by manual abdominal pressure every day until 2 weeks post-injury. Food and water were provided *ad libitum*. All animals were treated and cared for in accordance with the Chiba University School of Medicine guidelines pertaining to the treatment of experimental animals.

IFN-γ treatment

Immediately following SCI, the mice received an IP injection of 1.0×10^4 U recombinant mouse IFN-γ (R&D Systems, Minneapolis, MN) diluted in 500 μL phosphate-buffered saline (PBS) or 500 μL vehicle (PBS) as a control, every day for 14 days. Prior to IP injection, we expressed their bladders manually, and measured body weight and the amount of residual urine.

Behavioral analysis

Hindlimb motor function was evaluated using the Basso mouse scale (BMS) open field locomotor test, in which the scores range from 0 to 9. BMS scores were recorded at 1, 3, 5, 7, 10, 14, 21, 28, 35, and 42 days following SCI by two independent examiners. We assessed hindlimb motion, mainly in order to determine whether the mouse could coordinately move and step. If there were differences in the BMS score between the right and left hindlimbs, we took the average of the two scores.

Tissue preparation and immunohistochemistry

For immunohistochemistry, the animals were sacrificed and perfused with 4% paraformaldehyde in 0.2 M phosphate buffer (pH 7.4) at 10 days (early phase) and 6 weeks (chronic phase) post-injury, and preserved spinal cord tissues were collected. The whole spine was dissected out and post-fixed in 4% paraformaldehyde for 24 h at 4°C. Next, the spinal cord was removed from the vertebral column and retained for 48 h in 30% sucrose at 4°C for cryoprotection. The spinal cord was embedded in Tissue-Tek OCT obtained from Sakura Finetechnical Co. Ltd. (Tokyo, Japan), and immediately frozen on dry ice at −80 °C. A series of 20-μm sagittal sections as well as cross-sections were cut on a cryostat and mounted on poly-L-lysine (PLL)-coated Superfrost-Plus slides purchased from Matsunami Glass (Osaka, Japan), and desiccated overnight. After washing three times with PBS, all sections were blocked in PBS containing 5% goat serum and 0.3% Triton X-100 for 1 h at room temperature. The sections were then incubated with primary antibodies overnight at 4°C, washed three times with PBS, and incubated with fluorescein-conjugated secondary antibodies for 1 h at room temperature. The sections were then rinsed three times in PBS and mounted. For primary antibodies, we used monoclonal anti-CD11b (1:400; BD Biosciences Pharmingen, San Diego, CA), monoclonal anti-GFAP (1:500; Sigma-Aldrich, St. Louis, MO), monoclonal anti-CSPG (1:400; Sigma-Aldrich), and monoclonal anti-serotonin (1:400; Sigma-Aldrich). Luxol fast blue (LFB) staining of spinal cord cross-sections was performed in order to measure the area of spared myelinated nerve fibers in the white matter. Immunohistochemistry using each antibody was performed simultaneously to equalize the variability of staining, and all of the slides underwent LFB staining simultaneously to equalize the variability of staining.

Histological assessment

Using spinal cord sections collected 10 days post-injury, we examined the distribution of macrophages/microglia, reactive astrocytes, and the expression of CSPGs. Every fifth section of the central portion of the spinal cords was serially mounted. At least four samples, each at 80-μm intervals within 320 μm of the center of the lesion site, were mounted on a slide and evaluated by immunohistochemistry as described above.

Using spinal cord sections collected 6 weeks post-injury, we determined the number of regenerated or spared neuronal fibers by staining serotonin fibers. Descending serotonergic fibers mainly derived from the raphe-spinal tract are thought to be important for locomotor control (Deumens et al., 2005). To confirm the axonal regeneration/sparing induced by IFN-γ treatment, we performed immunohistochemistry for serotonin to count the number of serotonin-positive fibers. Every fourth section of the central portion of the spinal cords was serially mounted. At least four samples, each at an 80-μm interval within 320 μm of the center of the lesion site, were mounted on a slide and evaluated for serotonin immunohistochemistry as described above. Lines were drawn perpendicular to the long axis of the spinal cord at the epicenter, and at 1, 2, and 3 mm rostral and caudal to the epicenter. The number of serotonin-positive fibers that traversed each line was counted.

We also assessed re-myelination or spared myelin by LFB staining in transverse sections. At least four samples, each at an 80-μm interval within 320 μm, were isolated from the epicenter, as were segments 0.6 mm, 1.2 mm, and 1.8 mm rostral or caudal to the lesion epicenter.

The number of cells was determined by immunoreactivity (fluorescence intensity) using Scion Image computer analysis software (Scion Corporation, Medford, MA), and Photoshop 7.0 software (Adobe Systems, San Jose, CA).

Real-time quantitative polymerase chain reaction

Total RNA from the injured spinal cords (6-mm segments including the lesion epicenter; the samples were near the region assessed by immunohistochemistry) was isolated 1 week after SCI using an RNeasy Kit (Qiagen, Hilden, Germany), and cDNA was obtained using reverse transcriptase (GE Healthcare, Buckinghamshire, U.K.). For the quantitative analysis of mRNA expression of neurotrophic factors, proinflammatory cytokines, and neurocan, the cDNA was used as the template in a TaqMan real-time PCR assay (ABI Prism 7500 Sequence Detection System; Applied Biosystems, Foster City, CA), according to the manufacturer's protocol. Specific primers and probes for the TaqMan real-time PCR assay were purchased from Applied Biosystems. The following TaqMan probes were used in this study: MCP-1 (Applied Biosystems catalog no. Mm99999056_m1), CCR-2 (no. Mm99999051_gH), neurocan (no. Mm00484007_m1), GDNF (no. Mm00599849_m1), IGF-1 (no. Mm00439561_m1), BDNF (no. Mm00432069_m1), and NT-3 (no. Mm00435413_s1).

Enzyme-linked immunosorbent assay (ELISA)

Injured spinal cords (6-mm segments including the lesion epicenter; the sample was near the same region assessed by immunohistochemistry) were homogenized in homogenization buffer (50 mM Tris-HCl [pH 7.4], 150 mM NaCl, and 1% Triton X-100) containing a protease inhibitor cocktail (complete; Roche Diagnostics, Basel, Switzerland). Homogenates were cleared by centrifugation at 14,000 rpm for 10 min at 4°C. Protein concentration of the supernatants was measured with Bio-Rad Dc Protein Assay Reagents (Bio-Rad Laboratories, Hercules, CA), and the protein concentration was adjusted to 1 mg/mL by diluting the supernatants with a homogenization buffer. IFN-γ in the supernatants was quantified with an immunoassay kit from Bender MedSystems (Vienna, Austria), following the manufacturer's protocol. In order to determine if IP-administrated IFN-γ reached the injured spinal cord, we examined IFN-γ concentration with ELISA at 5, 10, and 14 days post-SCI.

Western blotting

Homogenates of injured spinal cords were prepared as described above in the ELISA section. After centrifugation, protein concentration of the supernatants was adjusted to 1 mg/mL. For the detection of neurocan, the supernatants were digested by chondroitinase ABC (Seikagaku Corp., Tokyo, Japan) for 3 h at 4°C, and mixed with an equal volume of a 2×sample buffer (250 mM Tris-HCl, 4% sodium dodecyl sulfate [SDS], 20% glycerol, 0.02% bromophenol blue, and 10% β-mercaptoethanol). For the detection of GFAP, Nogo A, and semaphorin 3A, the supernatants were mixed with an equal volume of a 2×sample buffer. After boiling for 5 min, equal volumes of the samples were subjected to 5% (neurocan) or 10% (GFAP, Nogo A, and semaphorin 3A) SDS-polyacrylamide gel electrophoresis (SDS-PAGE) under reducing conditions, and the proteins were transferred to a polyvinylidene difluoride membrane (Immobilon-P; Millipore Corp., Billerica, MA). After blocking of the membrane with PBS containing 5% skim milk and 0.05% Tween 20, the membrane was reacted with anti-neurocan (Seikagaku Corp.), anti-GFAP (Sigma-Aldrich), anti-Nogo A (Santa Cruz Biotechnology, Santa Cruz, CA), or anti-semaphorin 3A (Santa Cruz Biotechnology) antibodies. For detection, a horseradish peroxidase-conjugated secondary antibody (Cell Signaling Technology, Beverly, MA), and an ECL chemiluminescence system (GE Healthcare) were used. Quantification of protein bands was performed using Scion image software.

Astrocyte culture

Primary astrocyte cultures were prepared from newborn mice at post-natal day 1 (P1). The upper portion of the skull was opened and the meninges were carefully removed in order to minimize contamination of the cell culture with fibroblasts. The cerebral cortices were cut into small pieces and enzymatically dissociated using 0.025% trypsin in PBS for 10 min at 37°C. Following the addition of 10% FBS and 0.5 mg/mL DNase I, the dissociated cortices were triturated and then gravity filtered through a 70-μm cell strainer. The cells were resuspended in Dulbecco's modified Eagle's medium (DMEM) plus GlutaMAX (Invitrogen Corp., Carlsbad, CA) containing 10% fetal bovine serum (FBS) and 1% penicillin/streptomycin, and then seeded onto PLL-coated 75-cm^2 tissue culture flasks. The medium was changed every 3 days until the cells were confluent. Thereafter, the flasks were shaken at 200 rpm for 6 h in order to remove the contaminating non-astrocytic cells. The astrocytes were gently trypsinized, rinsed in fresh medium containing 10% FBS, and then plated on PLL-coated four-chamber glass slides. The astrocytes were treated with 10 ng/mL transforming growth factor-β (TGF-β), purchased from PeproTech, Inc. (Rocky Hill, NJ), or 10 ng/mL epidermal growth factor (EGF; PeproTech, Inc.), in the absence or presence of 2.0×10^3 U/mL IFN-γ (R&D Systems) for 24 h, before collection of total RNA using an RNeasy Kit (Qiagen).

Statistical analysis

For all experiments with the exception of the behavioral analyses, statistical analysis was performed using the Student's *t*-test. For the behavioral analyses, BMS scores were analyzed using repeated-measures analysis of variance (ANOVA), followed by Fisher's protected least significant difference (PLSD) *post-hoc* test. For fractional BMS scores at each time point, one-way ANOVA followed by the Bonferroni/Dunn test were used. Statistical significance was set at $p < 0.05$ for fractional BMS scores. All values are the means ± standard error.

Results

Intraperitoneally-administered IFN-γ reaches the injured spinal cord

We performed ELISA for IFN-γ to determine whether intraperitoneally-administered IFN-γ can reach the injured

spinal cord. IFN-γ was almost undetectable in uninjured and injured spinal cords without IFN-γ treatment. In contrast, IFN-γ was clearly detected in the injured spinal cords with IFN-γ treatment at 5 and 10 days post-SCI, suggesting that the intraperitoneally-administered IFN-γ had reached the injured spinal cords at least until 10 days post-SCI (Fig. 1).

IFN-γ improves locomotor performance post-SCI

In order to assess the therapeutic effects of IFN-γ on a mouse contusion SCI model, IP administration of IFN-γ once a day for 14 days post-SCI was performed. We evaluated the locomotor function of hindlimbs by recording BMS scores for up to 6 weeks post-SCI. The overall BMS scores for IFN-γ-treated mice were significantly higher than those of the vehicle-treated mice, as calculated by repeated-measures ANOVA ($p < 0.01$); furthermore, at specific time points (10, 14, and 21 days) post-SCI, there were significant differences between the two groups ($p < 0.05$; Fig. 2). After 6 weeks, the vehicle-treated group's score leveled off at 2.8 ± 0.6 points, while the IFN-γ-treated group was at 4.4 ± 0.6 points, and its score appeared to continue to increase. Whereas the hindlimbs of the vehicle-treated mice exhibited only extensive ankle movement, IFN-γ-treated mice exhibited occasional plantar stepping or consistent dorsal stepping within 10 days post-SCI, suggesting that IFN-γ has therapeutic effects, even in the early phase post-injury. We also examined body weight and residual urine; however, there were no significant differences between the two groups (data not shown).

IFN-γ treatment increased the range of macrophage/microglia accumulation post-SCI

The distribution of macrophages/microglia in spinal cords following injury was examined immunohistochemically at 10 days post-SCI. At this time point, numerous CD11b-positive macrophages/microglia were seen densely clustered in the epicenter of the injured area in vehicle-treated mice, as previously reported (Kigerl et al., 2006; Sroga et al., 2003; Fig. 3A). However, the injured spinal cords of IFN-γ-treated mice exhibited a different distribution of these cells. In these mice, the accumulation of macrophages/microglia was less dense at the epicenter; instead, these cells were more widely distributed from the rostral to the caudal side of the epicenter (Fig. 3B). The mean range of the horizontal distribution of the infiltrated macrophages/microglia was 1.18 ± 0.03 mm in the vehicle-treated group, and 6.15 ± 0.96 mm in the IFN-γ-treated group (Fig. 3D), and the difference between the two groups was statistically significant ($p < 0.05$). There was a tendency for more macrophages/microglia to accumulate in the IFN-γ-treated group; however, the difference between the two groups was not statistically significant ($p = 0.08$; Fig. 3C). We attempted to determine the difference in macrophage/microglia distribution by examining the expression of chemokines that are known to affect macrophage migration. We examined the mRNA levels of MCP-1 and its receptor CCR-2 in the spinal cord at 1 week post-SCI by real-time PCR (Fig. 3E and F). The relative levels of MCP-1 and CCR-2 mRNAs were 1.9 and 3.8 times higher, respectively, in the IFN-γ-treated group than in the vehicle-treated group. To address the effects of IFN-γ treatment on the levels of proinflammatory cytokines, we checked mRNA levels of TNF-α, IL-1β, and IL-6 in the spinal cord at 1 week post-SCI by real-time PCR (Supplementary Fig. 1; see online supplementary material at http://www.liebertonline.com). There was no statistically significant difference in the levels of TNF-α, IL-1β, and IL-6 mRNA with vehicle or IFN-γ treatment, although there was a tendency toward an increase in IL-1β and IL-6 levels with IFN-γ treatment.

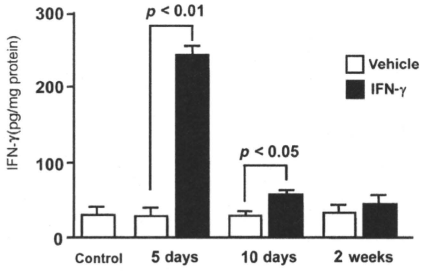

FIG. 1. Intraperitoneally-administered interferon-γ (IFN-γ) reached the injured spinal cord. We performed enzyme-linked immunosorbent assay (ELISA) for IFN-γ to determine whether intraperitoneally-administered IFN-γ could reach the injured spinal cord. IFN-γ was nearly undetectable in uninjured and injured spinal cords without IFN-γ treatment. In contrast, IFN-γ was clearly detected in the injured spinal cords with IFN-γ treatment at 5 and 10 days post-SCI, suggesting that the intraperitoneally-administered IFN-γ reached the injured spinal cords at least until 10 days post-SCI (SCI, spinal cord injury).

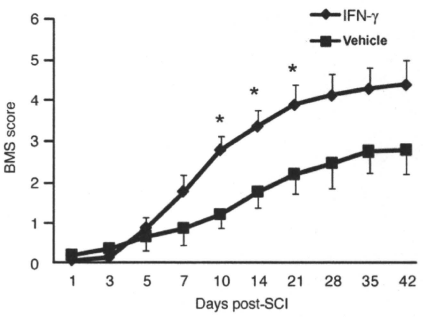

FIG. 2. Interferon-γ (IFN-γ) promotes functional recovery following spinal cord injury (SCI). Hindlimb function of mice following SCI was evaluated using the Basso mouse locomotor scale (BMS). Repetitive administration of IFN-γ for 14 days post-injury significantly enhanced hindlimb functional recovery, as assessed by repeated-measures analysis of variance (ANOVA; $p < 0.01$). After 10, 14, and 21 days post-SCI, IFN-γ-treated mice ($n = 15$) exhibited significantly better hindlimb function than vehicle-treated mice ($n = 13$; $^*p < 0.05$).

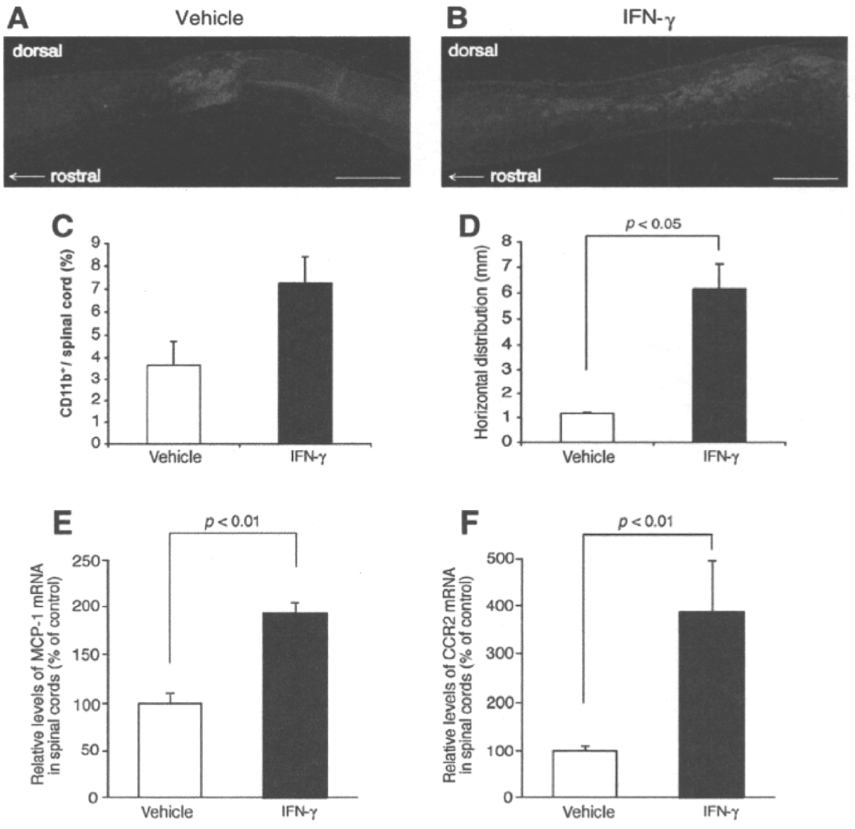

FIG. 3. Horizontal distribution of CD11b-positive macrophages/microglia in IFN-γ-treated mice post-SCI. Ten days post-SCI, the spinal cords of vehicle-treated (**A**) and IFN-γ-treated (**B**) mice were fixed and sagittal sections were stained with anti-CD11b antibody (scale bar = 1 mm). (**C**) The CD11b-positive area in a section including 5 mm rostral and caudal from the epicenter was measured, and is expressed as the percentage of CD11b-positive area relative to the total area examined. There was no statistically significant difference between the vehicle-treated group ($3.7 \pm 1.1\%$), and the IFN-γ-treated group ($7.3 \pm 1.1\%$; $p = 0.08$). (**D**) The length of the horizontal distribution of CD11b-positive cells was measured. Six spinal cord sections per animal and three animals from each group were included in the assessment. There was a statistically significant difference between the vehicle-treated group (1.18 ± 0.03 mm), and the IFN-γ-treated group (6.15 ± 0.96 mm; $p < 0.05$). Quantitative RT-PCR for MCP-1 (**E**) and CCR2 (**F**) was performed by using mRNA isolated from 6-mm-long sections of injured spinal cords including the lesion center at the middle ($n = 3$). Injured spinal cords were dissected 7 days post-SCI (IFN-γ, interferon-γ; SCI, spinal cord injury; RT-PCR, real-time polymerase chain reaction).

IFN-γ treatment decreases the accumulation of CSPG post-SCI

Following SCI, reactive astrocytes accumulate around the epicenter of the injured spinal cord and express molecules that inhibit axonal regeneration. Therefore, we examined the distribution of reactive astrocytes at 10 days post-SCI. Consistent with a previous report (Popovich et al., 1997), reactive astrocytes were detected in the tissue circumscribing the wound cavity at the lesion center (Fig. 4A and B). In the vehicle-treated group, GFAP staining was highest at the lesion edge and sharply decreased rostrally and caudally (Fig. 4A). In contrast, elevated GFAP staining in the IFN-γ-treated group had extended rostrally and caudally (Fig. 4B). Consistent with this observation, quantification of GFAP-positive immunoreactivity revealed that the accumulated reactive astrocytes were significantly higher rostrally and caudally in the IFN-γ-treated group than in the control group, except at the epicenter (Fig. 4C).

Next, we used immunohistochemistry to analyze the expression of CSPGs, which are the major axon growth inhibitors that accumulate following CNS injury, and which are mainly produced by reactive astrocytes (Fig. 5A–D). The CSPG signals were detected around the wound cavity at the epicenter. The distribution of immunoreactivity for CSPGs was similar to that of the GFAP-positive reactive astrocytes, as expected (McKeon et al., 1991, 1999; Smith and Strunz, 2005; Yiu and He, 2006). The mean density of CSPGs was significantly reduced in the IFN-γ-treated group ($0.57 \pm 0.05\%$), compared to the vehicle-treated group ($1.16 \pm 0.07\%$), suggesting that IFN-γ treatment decreased the accumulation of CSPGs following SCI in mice (data not shown). In addition, we measured the horizontal distribution of CSPG expression by quantification of immunoreactivity for CSPG. In the vehicle-treated group, CSPG staining was highest at the lesion edge, and sharply decreased rostrally and caudally (Fig. 5E). In contrast, elevated CSPG staining in the IFN-γ-treated group extended rostrally and caudally (Fig. 5E). Horizontal distribution of CSPG immunoreactivity was similar to that of GFAP (Fig. 4A–E). To directly examine whether the levels of CSPG production were reduced by IFN-γ treatment, we analyzed the mRNA

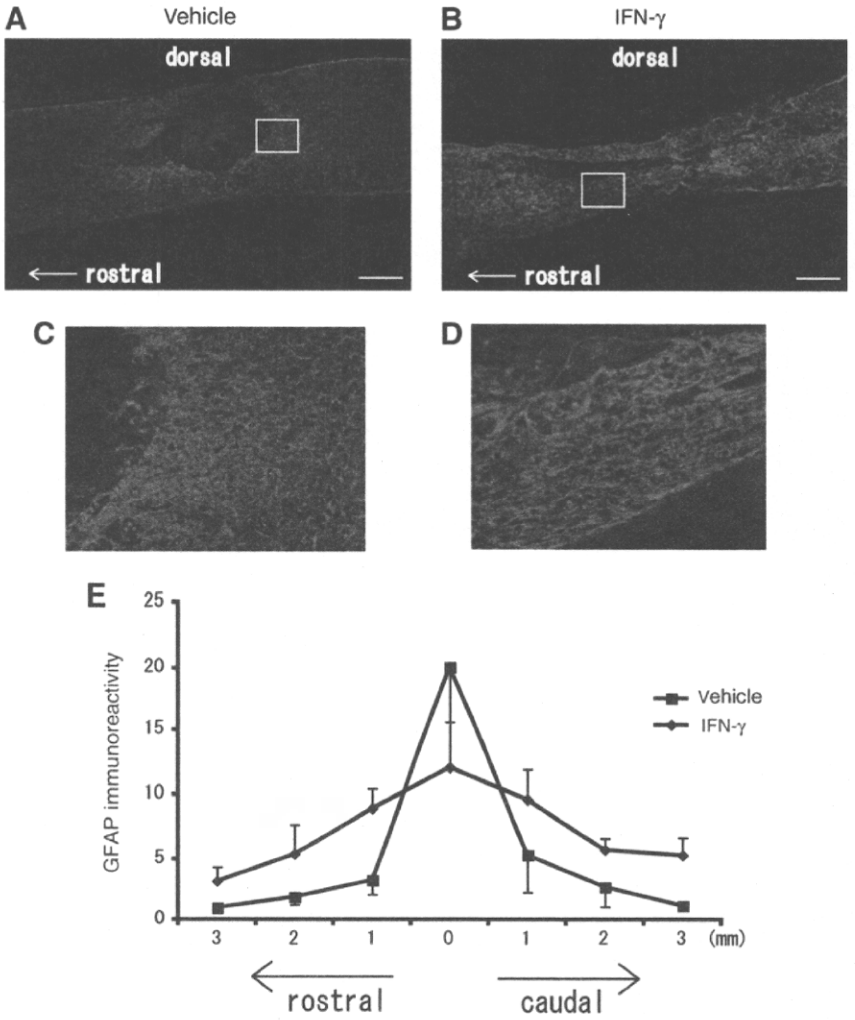

FIG. 4. Accumulation of glial fibrillary acidic protein (GFAP)-positive reactive astrocytes post-SCI. At 10 days post-SCI, the spinal cords of vehicle-treated (**A** and **C**), and IFN-γ-treated (**B** and **D**) mice were fixed and sagittal sections were immunolabeled with anti-GFAP antibody (scale bar = 400 μm). (**E**) The GFAP immunoreactivity was quantified rostrally and caudally from the lesion center at 1-mm intervals, and is expressed as the relative ratio to that of control animals at 3 mm rostral. There was a statistically significant difference between the control group and the IFN-γ-treated group, except at the epicenter ($p < 0.05$; IFN-γ, interferon-γ; SCI, SCI, spinal cord injury).

and protein levels of neurocan, one of the CSPGs that is typically upregulated following CNS injury, in injured spinal cords by quantitative RT-PCR and Western blotting, respectively. IFN-γ treatment significantly reduced the levels of neurocan in the tissues surrounding the lesion epicenter at 7 days post-SCI at both mRNA and protein levels (Fig. 6A and B). Since reactive astrocytes are considered to be a major source of CSPGs post-CNS injury, we evaluated the effects of IFN-γ on neurocan expression by stimulated astrocytes *in vitro* (Fig. 6C and D). It has been reported that TGF-β and EGF enhance the expression of GFAP and neurocan in cultured astrocytes as pathologically relevant stimulators, and mimic the molecular events occurring in reactive astrocytes in the injured spinal cord (Asher et al., 2000; Smith and Strunz, 2005). Therefore, we evaluated the effects of IFN-γ on TGF-β- or EGF-induced expression of neurocan in cultured astrocytes. IFN-γ significantly decreased the levels of neurocan mRNA in TGF-β- or EGF-treated astrocytes (Fig. 6C). In addition, IFN-γ cancelled the TGF-β-induced upregulation of neurocan protein expression, whereas IFN-γ treatment had no influence on TGF-β-induced GFAP expression enhancement (Fig. 6D). However, IFN-γ had no significant effect on EGF-induced neurocan upregulation (data not shown). These data suggest that IFN-γ treatment may block the upregulation of CSPGs in activated astrocytes at the transcriptional level.

IFN-γ had no effect on the levels of other axon growth inhibitors

We analyzed whether IFN-γ modulated the levels of other axon growth inhibitors such as semaphorin 3A and Nogo A, both of which were reported to be upregulated and involved in the deficit of axonal recovery post-SCI, by Western blotting. IFN-γ exhibited no effects on the levels of either protein in injured spinal cords at 5, 10, and 14 days post-SCI (data not shown).

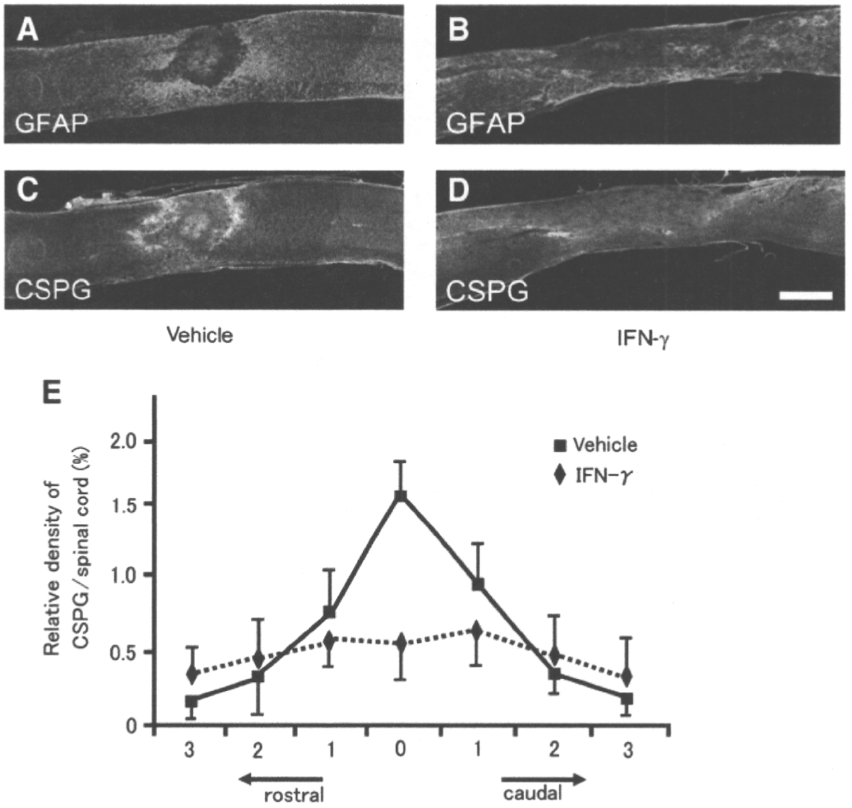

FIG. 5. Interferon-γ (IFN-γ) alters chondroitin sulfate proteoglycan (CSPG) distribution post-SCI. At 10 days post-SCI, the spinal cords of vehicle-treated (**A** and **C**), and IFN-γ-treated (**B** and **D**) mice, were fixed and parasagittal sections were stained with anti-GFAP antibody (**A** and **B**), and anti-CSPG antibody (**C** and **D**; scale bar = 500 μm). Note that the distribution of the CSPG signals (green) is similar to that of the GFAP signals (red). (**E**) Quantification of CSPG expression. The method of measurement was the same as for the quantification of GFAP expression shown in Figure 4E (GFAP, glial fibrillary acidic protein; SCI, spinal cord injury).

IFN-γ treatment increased 5-HT-positive fibers around the epicenter following SCI

Since the serotonergic raphe-spinal neuronal circuit contributes to locomotor function (Kim et al., 2004), we examined serotonergic fiber sprouting by 5-HT immunostaining at 6 weeks post-SCI. Numerous 5-HT-positive fibers were found close to the lesion cavity of injured spinal cords in IFN-γ-treated mice (Fig. 7C and D), whereas few positive fibers were detected in the vehicle-treated mice (Fig. 7A and B). The number of fibers was counted at 1-mm intervals rostrally or caudally from the lesion center. The number of 5-HT-positive fibers was significantly higher at the center and 1 mm rostral to the lesion center in the IFN-γ-treated group ($p < 0.05$) (Fig. 7E), suggesting that IFN-γ treatment either enhances the growth of serotonergic nerve fibers or was neuroprotective following SCI.

IFN-γ treatment increased the area of spared myelin

We performed Luxol fast blue (LFB) staining at 6 weeks post-SCI, and assessed the percentage of LFB-positive myelinated area relative to the total area of white matter. In both groups, the highest degree of demyelination occurred at the epicenter, and the area of spared myelin gradually increased rostrally and caudally (Fig. 8A). As shown in Figure 8B and C, IFN-γ treatment increased the myelinated area, and there was a significant difference between the two groups at 1.8 mm rostral and 0.6 mm caudal to the epicenter (Fig. 8A). The percentage of the myelinated area was 37.3 ± 1.5% in the vehicle-treated group, and 48.1 ± 1.6% in the IFN-γ-treated group, at 1.8 mm rostral to the epicenter, and 23.9 ± 2.0% in the vehicle-treated group, and 40.2 ± 2.6% in the IFN-γ-treated group, at 0.6 mm caudal to the epicenter (Fig. 8A). These data demonstrate that IFN-γ treatment increased the sparing of myelinated fibers post-SCI in mice.

IFN-γ treatment increased the expression of neurotrophic factors post-SCI

Since IFN-γ treatment increased the 5-HT-positive nerve fibers and enhanced sparing of myelinated fibers following SCI, we hypothesized that IFN-γ regulates the levels of certain neurotrophic factors post-SCI. We found that glial cell line-derived neurotrophic factor (GDNF) and insulin growth factor-1 (IGF-1) mRNA levels were significantly upregulated in the tissues surrounding the lesion epicenter in the IFN-γ-treated group, compared with those of the vehicle-treated group, whereas the levels of brain-derived neurotrophic factor (BDNF) and neurotrophin-3 (NT-3) mRNA were about the same in the two groups (Fig. 9A).

Discussion

In the present study, we demonstrated that IFN-γ exhibits therapeutic effects in an experimental mouse contusion SCI

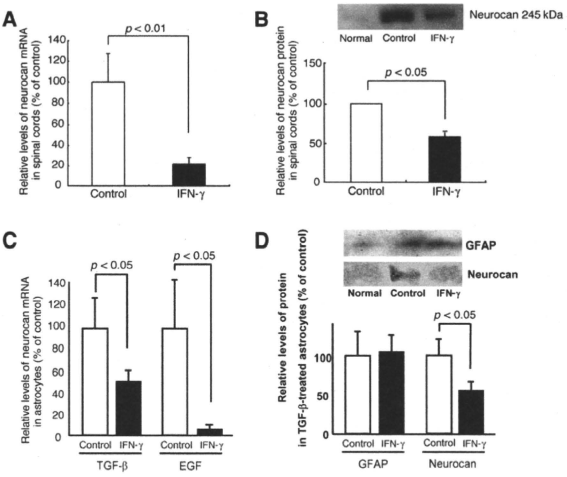

FIG. 6. Interferon-γ (IFN-γ) reduces chondroitin sulfate proteoglycan (CSPG) accumulation post-SCI. In order to analyze the levels of neurocan mRNA (**A**) and protein (**B**) in injured spinal cords with and without IFN-γ treatment, quantitative RT-PCR and Western blotting were performed ($n = 3$–6). (**C**) In the presence of TGF-β or EGF, cultured astrocytes were exposed to IFN-γ or vehicle (PBS) for 24 h, and the effects of IFN-γ on the levels of neurocan mRNA were analyzed by quantitative RT-PCR ($n = 3$–5). (**D**) TGF-β-treated astrocytes were exposed to IFN-γ or vehicle, protein was extracted, and Western blot analysis was performed to detect GFAP and neurocan. IFN-γ inhibited TGF-β-induced upregulation of neurocan protein expression (RT-PCR, real-time polymerase chain reaction; TFG-β, transforming growth factor-β; EGF, epidermal growth factor; GFAP, glial fibrillary acidic protein; SCI, spinal cord injury).

model, which is one of the clinically relevant animal models of SCI. To the best of our knowledge, this is the first study to demonstrate the therapeutic effects of IFN-γ on SCI. The IP administration of IFN-γ promoted significant functional recovery as early as 10 days post-SCI, suggesting that IFN-γ therapy could be valuable in the clinical setting. Notably, the hindlimbs of IFN-γ-treated mice displayed plantar stepping, whereas vehicle-treated mice could only move their ankles. In order to identify the anatomical basis for the functional recovery seen in IFN-γ-treated mice post-SCI, we initially attempted to trace the corticospinal tract by biotin dextran amine labeling; however, we were unable to obtain stable labeling in our mouse contusion SCI model. Therefore, we assessed the growth of 5-HT-positive raphe-spinal fibers, which are associated with locomotor recovery post-SCI (Kim et al., 2004). Consistent with the functional recovery seen in the IFN-γ-treated mice, we detected an increase in 5-HT-positive neuronal fibers following IFN-γ administration. In addition, we detected an increase in spared myelinated fibers in the white matter around the epicenter of the injured spinal cord in these mice. It has been reported that an increase in 5-HT-positive fibers and myelinated fibers strongly correlates with functional recovery post-SCI (Fouad et al., 2005; Kim et al., 2004; Oatway et al., 2005).

Although it remains to be determined how IFN-γ treatment promotes the growth of the neuronal axons and myelin sparing seen post-SCI, the decreased accumulation of axon growth inhibitors and increase in neurotrophic factors around the injured spinal cords in IFN-γ-treated mice may, at least partly, contribute to the enhanced restoration. In the present study, we found that IFN-γ treatment post-SCI significantly reduced the levels of CSPGs around the epicenter of injured spinal cords, with almost no effect on the number of reactive astrocytes, which are considered to be cellular sources of CSPGs. It is well established that the degradation of CSPGs by exogenously-administered chondroitinase ABC enhances histological and functional recovery post-SCI (Barritt et al., 2006; Bradbury et al., 2002). Therefore, it has been suggested that the IFN-γ-induced reduction of CSPG accumulation seen post-SCI creates an environment within the injured spinal cord that is conducive to axon growth. In addition to the immunohistochemical analyses, quantitative RT-PCR and Western blotting demonstrated that IFN-γ treatment suppressed the upregulation of neurocan mRNA and protein, which is one of CSPGs that is upregulated post-SCI, in injured spinal cords. This result suggests that IFN-γ treatment downregulates the levels of neurocan post-SCI at the transcriptional level. Consistent with this observation, neurocan mRNA in TGF-β- and EGF-treated astrocytes *in vitro* was significantly reduced by IFN-γ treatment (Fig. 6C), as has been demonstrated in previous studies (Asher et al., 2000; Smith and Strunz, 2005). In addition, IFN-γ inhibited the TGF-β-induced upregulation of neurocan protein

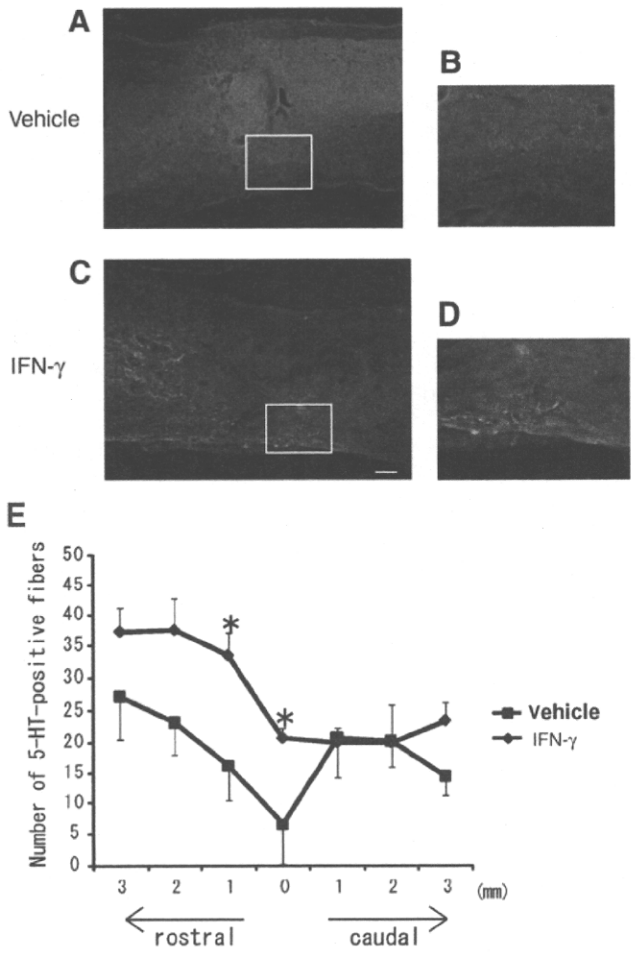

FIG. 7. Interferon-γ (IFN-γ) increases the number of 5-HT-positive fibers post-SCI. At 6 weeks post-SCI, the spinal cords of vehicle-treated (**A** and **B**) and IFN-γ-treated (**C** and **D**) mice were fixed, and sagittal sections were stained with anti-5-HT antibody. At the lesion center, higher-magnification images of the white boxes in **A** and **C** are shown in **B** and **D** (scale bar = 200 μm). (**E**) The numbers of 5-HT-positive fibers that crossed lines perpendicular to the central axis of the spinal cords were counted. The lines were positioned rostrally and caudally from the lesion center at 1-mm intervals. The number of 5-HT-positive fibers was significantly higher in IFN-γ-treated mice than in control mice at the lesion center and 1 mm rostral from the epicenter (*$p < 0.05$; 5-HT, serotonin; SCI, spinal cord injury).

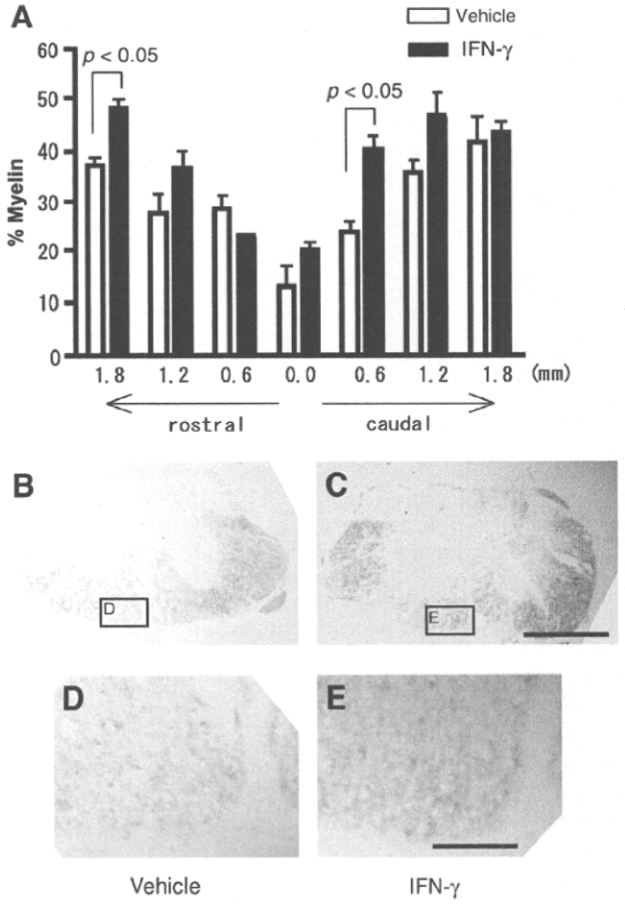

FIG. 8. Interferon-γ (IFN-γ) increases sparing of myelinated fibers post-SCI. At 6 weeks post-SCI, Luxol fast blue (LFB) staining of cross-sections of spinal cords was performed in order to analyze the effects of IFN-γ treatment on the levels of myelinated fibers seen post-SCI. (**A**) Graph showing the percentage of myelinated area relative to the total area of white matter in the cross-sections. We also assessed remyelination or spared myelin by LFB staining in transverse sections. At least four samples, each at an 80-μm interval within 320 μm were isolated from the epicenter, and at 0.6 mm, 1.2 mm, and 1.8 mm rostral or caudal to the lesion epicenter. The number of myelinated fibers in the IFN-γ-treated group tended to be greater than in the control group, and the difference between the two groups at 1.8 mm rostral and 0.6 mm caudal from the center reached statistical significance ($p < 0.05$). (**B** and **C**) Representative LFB-stained cross sections at 400 μm caudal from the lesion center of vehicle-treated (**B** and **D**) and IFN-γ-treated (**C** and **E**) spinal cords are shown. The myelinated fibers were more dense in the IFN-γ-treated mice than in the vehicle-treated mice (SCI, spinal cord injury).

expression, whereas IFN-γ treatment had no influence on TGF-β-induced GFAP expression enhancement (Fig. 6D). GFAP upregulation is thought to be one of the manifestations of astrocyte activation. Thus IFN-γ treatment does not suppress the astrocyte activation itself, but suppresses CSPG upregulation. However, IFN-γ had no significant effect on EGF-induced neurocan upregulation. The precise mechanism underlying the discrepancy in the influence of IFN-γ between neurocan mRNA and protein expression in EGF-stimulated astrocytes is still unclear. These results suggest that IFN-γ treatment suppresses the upregulation of CSPGs at the transcriptional level post-SCI, by modulating the function of reactive astrocytes. The reduction of CSPGs by IFN-γ treatment in the injured spinal cord is relatively specific, since we observed that the levels of other axon growth inhibitors, such as semaphorin 3A and Nogo A, did not change with IFN-γ treatment.

IFN-γ also modulates the functions of macrophages/microglia post-SCI. We found that IFN-γ administration induced a widespread distribution of macrophages/microglia post-SCI. One possible mechanism by which IFN-γ alters macrophage/microglia distribution is via the IFN-γ-induced expression of chemokines such as IL-10, RANTES, and MCP-1,

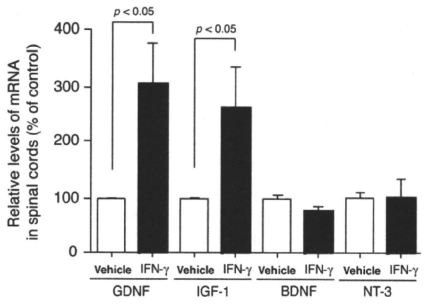

FIG. 9. Interferon-γ (IFN-γ) increases levels of neurotrophic factors post-SCI. The effects of IFN-γ on the expression levels of neurotrophic factors post-SCI were examined by quantitative RT-PCR for the indicated neurotrophic factors, as described in the legend to Figure 3 ($n = 3$; SCI, spinal cord injury; RT-PCR, real-time polymerase chain reaction; GDNF, glial cell line-derived neurotrophic factor (GDNF; IGF-1, insulin growth factor-1, BDNF, brain-derived neurotrophic factor; BNT-3, neurotrophin-3).

all of which promote the migration of macrophages into inflamed tissues (Schroder et al., 2004). In this context, we detected an upregulation of the mRNAs of MCP-1 and its receptor CCR2 in the IFN-γ-treated group at 7 days post-injury (Fig. 3E and F). Although the correlation between the IFN-γ-induced extensive accumulation of macrophages/microglia and the therapeutic effects of IFN-γ on SCI remain uncertain, the accumulation of macrophages/microglia induced by IFN-γ might produce effector molecules that support neuronal recovery post-SCI. Among these molecules, probable candidates for the promotion of neuronal recovery post-SCI are the IFN-γ-induced neurotrophic factors. It has been reported that activated macrophages/microglia produce several neurotrophic factors, such as NT-3, IGF-1, GDNF, and BDNF (Donnelly and Popovich, 2008; Elkabes et al., 1996; Hashimoto et al., 2005a, 2005b; Kaur et al., 2006; Nakajima et al., 2001). In this study, we detected an increase in the mRNAs of GDNF and IGF-1 with IFN-γ treatment post-SCI (Fig. 9). It is well established that these neurotrophic factors promote axon elongation and functional recovery post-SCI (Cheng et al., 2002; Grill et al., 1997; Iannotti et al., 2003; Sharma, 2005; Zhou et al., 2003). In this context, it has recently been proposed that IGF-1 is one of the axon-promoting factors of corticospinal motor neurons, the damage to which causes dysfunction of hindlimb movement in SCI models (Ozdinler and Macklis, 2006). In addition, these neurotrophic factors are reported to enhance the remyelination of PNS and CNS neuronal fibers in several experimental animal models (Blesch and Tuszynski, 2003; Girard et al., 2005; Mason et al., 2003; McTigue et al., 1998). These findings are consistent with our observation that IFN-γ treatment increases spared myelin post-SCI. At present, the cellular source of neurotrophic factors that are upregulated by IFN-γ treatment remains unclear. Our preliminary experiments showed that IFN-γ induces increased GDNF production by bone marrow-derived macrophages (BMDMs). In contrast, IFN-γ induced only a slight upregulation of GDNF expression by cultured microglia. Thus the main cellular source of GDNF may be macrophages. As for IGF-1, certain doses of IFN-γ can suppress IGF-1 expression in cultured microglia (Butovsky et al., 2006), and BMDMs. Therefore IFN-γ-mediated IGF-1 upregulation may be attributable to an interaction between IFN-γ-stimulated macrophages/microglia and the other cellular source within the spinal cord.

In the present study, we demonstrated that IFN-γ reduces the accumulation of CSPGs and enhances the production of GDNF and IGF-1 *in vivo* following SCI. Importantly, IFN-γ significantly promoted functional recovery following SCI in this experimental setting. The dose, timing, and duration of IFN-γ treatment should have a strong influence on its therapeutic effects. In a different setting, IFN-γ treatment might worsen the inflammatory reaction and exacerbate the paralysis resulting from SCI. Thus further exploration is needed to establish its optimal therapeutic regimen.

At present, the pharmacotherapeutic treatments available for human SCI are extremely limited. Since IFN-γ is currently used for the treatment of mycosis fungoides in humans, it would be of interest to test the therapeutic effects of clinically-available IFN-γ on patients with SCI.

Acknowledgments

We are grateful to Drs. T. Yamashita (Osaka University), and M. Hashimoto, Y. Someya, R. Kadota, C. Mannoji, T. Miyashita, J. Kawabe, T. Furuya, T. Endo, and K. Hayashi (Chiba University), for their helpful comments on this manuscript. This work was supported by a research grant from a Grant-in-Aid for Young Scientists (start-up) from Japan Society for the Promotion of Science (JSPS), and a research grant from the Futaba Electronics Memorial Foundation to T.K.

Author Disclosure Statement

No competing financial interests exist.

References

Asher, R.A., Morgenstern, D.A., Fidler, P.S., Adcock, K.H., Oohira, A., Braistead, J.E., Levine, J.M., Margolis, R.U., Rogers, J.H., and Fawcett, J.W. (2000). Neurocan is upregulated in injured brain and in cytokine-treated astrocytes. J. Neurosci. 20, 2427–2438.

Barritt, A.W., Davies, M., Marchand, F., Hartley, R., Grist, J., Yip, P., McMahon, S.B., and Bradbury, E.J. (2006). Chondroitinase ABC promotes sprouting of intact and injured spinal systems after spinal cord injury. J. Neurosci. 26, 10856–10867.

Blesch, A., and Tuszynski, M.H. (2003). Cellular GDNF delivery promotes growth of motor and dorsal column sensory axons after partial and complete spinal cord transections and induces remyelination. J. Comp. Neurol. 467, 403–417.

Bradbury, E.J., Moon, L.D., Popat, R.J., King, V.R., Bennett, G.S., Patel, P.N., Fawcett, J.W., and McMahon, S.B. (2002). Chondroitinase ABC promotes functional recovery after spinal cord injury. Nature 416, 636–640.

Butovsky, O., Ziv, Y., Schwartz, A., Landa, G., Talpalar, A.E., Pluchino, S., Martino, G., and Michal Schwartz, M. (2006). Microglia activated by IL-4 or IFN-γ differentially induce neurogenesis and oligodendrogenesis from adult stem/progenitor cells. Mol. Cell. Neurosci. 31, 149–160.

Cheng, H., Wu, J.P., and Tzeng, S.F. (2002). Neuroprotection of glial cell line-derived neurotrophic factor in damaged spinal cords following contusive injury. J. Neurosci. Res. 69, 397–405.

Deumens, R., Koopmans, G.C., and Joosten, E.A. (2005). Regeneration of descending axon tracts after spinal cord injury. Prog. Neurobiol. 77, 57–89.

Donnelly, D.J., and Popovich, P.G. (2008). Inflammation and its role in neuroprotection, axonal regeneration and functional recovery after spinal cord injury. Exp. Neurol. 209, 378–388.

Elkabes, S., DiCicco-Bloom, E.M., and Black, I.B. (1996). Brain microglia/macrophages express neurotrophins that selectively regulate microglial proliferation and function. J. Neurosci. 16, 2508–2521.

Fouad, K., Schnell, L., Bunge, M.B., Schwab, M.E., Liebscher, T., and Pearse, D.D. (2005). Combining Schwann cell bridges and olfactory-ensheathing glia grafts with chondroitinase promotes locomotor recovery after complete transection of the spinal cord. J. Neurosci. 25, 1169–1178.

Genovese, T., Mazzon, E., Crisafulli, C., Di Paola, R., Muià, C., Bramanti, P., and Cuzzocrea, S. (2006). Immunomodulatory effects of etanercept in an experimental model of spinal cord injury. J. Pharmacol. Exp. Ther. 316, 1006–1016.

Girard, C., Bemelmans, A.P., Dufour, N., Mallet, J., Bachelin, C., Nait-Oumesmar, B., Baron-Van Evercooren, A., and Lachapelle, F. (2005). Grafts of brain-derived neurotrophic factor and neurotrophin 3-transduced primate Schwann cells lead to functional recovery of the demyelinated mouse spinal cord. J. Neurosci. 25, 7924–7933.

Grill, R., Murai, K., Blesch, A., Gage, F.H., and Tuszynski, M.H. (1997). Cellular delivery of neurotrophin-3 promotes corticospinal axonal growth and partial functional recovery after spinal cord injury. J. Neurosci. 17, 5560–5572.

Hashimoto, M., Nitta, A., Fukumitsu, H., Nomoto, H., Shen, L., and Furukawa, S. (2005b). Inflammation-induced GDNF improves locomotor function after spinal cord injury. Neuroreport 16, 99–102.

Hashimoto, M., Nitta, A., Fukumitsu, H., Nomoto, H., Shen, L., and Furukawa, S. (2005a). Involvement of glial cell line-derived neurotrophic factor in activation processes of rodent macrophages. J. Neurosci. Res. 79, 476–487.

Iannotti, C., Li, H., Yan, P., Lu, X., Wirthlin, L., and Xu, X.M. (2003). Glial cell line-derived neurotrophic factor-enriched bridging transplants promote propriospinal axonal regeneration and enhance myelination after spinal cord injury. Exp. Neurol. 183, 379–393.

Jones, T.B., McDaniel, E.E., and Popovich, P.G. (2005). Inflammatory-mediated injury and repair in the traumatically injured spinal cord. Curr. Pharm. Des. 11, 1223–1236.

Kaur, C., Sivakumar, V., Dheen, S.T., and Ling, E.A. (2006). Insulin-like growth factor I and II expression and modulation in amoeboid microglial cells by lipopolysaccharide and retinoic acid. Neuroscience 138, 1233–1244.

Kigerl, K.A., McGaughy, V.M., and Popovich, P.G. (2006). Comparative analysis of lesion development and intraspinal inflammation in four strains of mice following spinal contusion injury. J. Comp. Neurol. 494, 578–594.

Kim, J.E., Liu, B.P., Park, J.H., and Strittmatter, S.M. (2004). Nogo-66 receptor prevents raphespinal and rubrospinal axon regeneration and limits functional recovery from spinal cord injury. Neuron 44, 439–451.

Koda, M., Nishio, Y., Kamada, T., Someya, Y., Okawa, A., Mori, C., Yoshinaga, K., Okada, S., Moriya, H., and Yamazaki, M. (2007). Granulocyte colony-stimulating factor (G-CSF) mobilizes bone marrow-derived cells into injured spinal cord and promotes functional recovery after compression-induced spinal cord injury in mice. Brain Res. 1149, 223–231.

Lazarov-Spiegler, O., Solomon, A.S., Zeev-Brann, A.B., Hirschberg, D.L., Lavie, V., and Schwartz, M. (1996). Transplantation of activated macrophages overcomes central nervous system regrowth failure. FASEB J. 10, 1296–1302.

Lee, Y.B., Yune, T.Y., Baik, S.Y., Shin, Y.H., Du, S., Rhim, H., Lee, E.B., Kim, Y.C., Shin, M.L., Markelonis, G.J., and Oh, T.H. (2000). Role of tumor necrosis factor-alpha in neuronal and glial apoptosis after spinal cord injury. Exp. Neurol. 166, 190–195.

Mason, J.L., Xuan, S., Dragatsis, I., Efstratiadis, A., and Goldman, J.E. (2003). Insulin-like growth factor (IGF) signaling through type 1 IGF receptor plays an important role in remyelination. J. Neurosci. 23, 7710–7718.

McKeon, R.J., Jurynec, M.J., and Buck, C.R. (1999). The chondroitin sulfate proteoglycans neurocan and phosphacan are expressed by reactive astrocytes in the chronic CNS glial scar. J. Neurosci. 19, 10778–10788.

McKeon, R.J., Schreiber, R.C., Rudge, J.S., and Silver, J. (1991). Reduction of neurite outgrowth in a model of glial scarring following CNS injury is correlated with the expression of inhibitory molecules on reactive astrocytes. J. Neurosci. 11, 3398–3411.

McTigue, D.M., Horner, P.J., Stokes, B.T., and Gage, F.H. (1998). Neurotrophin-3 and brain-derived neurotrophic factor induce oligodendrocyte proliferation and myelination of regenerating axons in the contused adult rat spinal cord. J. Neurosci. 18, 5354–5365.

Nakajima, K., Honda, S. Tohyama, Y., Imai, Y., Kohsaka, S., and Kurihara, T. (2001). Neurotrophin secretion from cultured microglia. J. Neurosci. Res. 65, 322–331.

Nesic, O., Xu, G.Y., McAdoo, D., High, K.W., High, K.W., Hulsebosch, C., and Perez-Pol, R. (2001). IL-1 receptor antagonist prevents apoptosis and caspase-3 activation after spinal cord injury. J. Neurotrauma 18, 947–956.

Nishio, Y., Koda, M., Kamada, T., Someya, Y., Kadota, R., Mannoji, C., Miyashita, T., Okada, S., Okawa, A., Moriya, H., and Yamazaki, M. (2007). Granulocyte colony-stimulating factor attenuates neuronal death and promotes functional recovery after spinal cord injury in mice. J. Neuropathol. Exp. Neurol. 66, 724–731.

Oatway, M.A., Chen, Y., Bruce, J.C., Dekaban, G.A., and Weaver, L.C. (2005). Anti-CD11d integrin antibody treatment restores normal serotonergic projections to the dorsal, intermediate, and ventral horns of the injured spinal cord. J. Neurosci. 25, 637–647.

Ozdinler, P.H., and Macklis, J.D. (2006). IGF-I specifically enhances axon outgrowth of corticospinal motor neurons. Nat. Neurosci. 9, 1371–1381.

Popovich, P.G., and Longbrake, E.E. (2008). Can the immune system be harnessed to repair the CNS? Nat. Rev. Neurosci. 9, 481–493.

Popovich, P.G., Wei, P., and Stokes, B.T. (1997). Cellular inflammatory response after spinal cord injury in Sprague-Dawley and Lewis rats. J. Comp. Neurol. 377, 443–464.

Rapalino, O., Lazarov-Spiegler, O., Agranov, E., Velan, G.J., Yoles, E., Fraidakis, M., Solomon, A., Gepstein, R., Katz, A., Belkin, M., Hadani, M., and Schwartz, M. (1998). Implantation of stimulated homologous macrophages results in partial recovery of paraplegic rats. Nat. Med. 4, 814–821.

Schroder, K., Hertzog, P.J., Ravasi, T., and Hume, D.A. (2004). Interferon-gamma: an overview of signals, mechanisms and functions. J. Leukoc. Biol. 75, 163–189.

Schwartz, M., Moalem, G., Leibowitz-Amit, R., and Cohen, I.R. (1999). Innate and adaptive immune responses can be beneficial for CNS repair. Trends. Neurosci. 22, 295–299.

Sharma, H.S. (2005). Neuroprotective effects of neurotrophins and melanocortins in spinal cord injury: an experimental study in the rat using pharmacological and morphological approaches. Ann. NY Acad. Sci. 1053, 407–421.

Shechter, R., London, A., Varol, C., Raposo, C., Cusimano, M., Yovel, G., Rolls, A., Mack, M., Pluchino, S., Martino, G., Jung, S., and Schwartz, M. (2009). Infiltrating blood-derived macrophages are vital cells playing an anti-inflammatory role in recovery from spinal cord injury in mice. PLoS Med. 6, e1000113.

Smith, G.M., and Strunz, C. (2005). Growth factor and cytokine regulation of chondroitin sulfate proteoglycans by astrocytes. Glia 52, 209–218.

Sroga, J.M., Jones, T.B., Kigerl, K.A., McGaughy, V.M., and Popovich, P.G. (2003). Rats and mice exhibit distinct inflammatory reactions after spinal cord injury. J. Comp. Neurol. 462, 223–240.

Stirling, D.P., Liu, S., Kubes, P., and Yong, V.W. (2009). Depletion of Ly6G/Gr-1 leukocytes after spinal cord injury in mice alters wound healing and worsens neurological outcome. J. Neurosci. 29, 753–764.

Yiu, G., and He, Z. (2006). Glial inhibition of CNS axon regeneration. Nat. Rev. Neurosci. 7, 617–627.

Zhou, L., Baumgartner, B.J., Hill-Felberg, S.J., McGowen, L.R., and Shine, H.D. (2003). Neurotrophin-3 expressed in situ induces axonal plasticity in the adult injured spinal cord. J. Neurosci. 23, 1424–1231.

Address correspondence to:
Masashi Yamazaki, M.D.
Department of Orthopaedic Surgery
Graduate School of Medicine
Chiba University
1-8-1 Inohana, Chuo-ku
Chiba 260-8677, Japan

E-mail: masashiy@faculty.chiba-u.jp

NEUROPATHOLOGY

Neuropathology 2011; **31**, 48–58 doi:10.1111/j.1440-1789.2010.01130.x

Original Article

Transplantation of human bone marrow stromal cell-derived Schwann cells reduces cystic cavity and promotes functional recovery after contusion injury of adult rat spinal cord

Takahito Kamada,[1] Masao Koda,[4] Mari Dezawa,[5] Reiko Anahara,[2] Yoshiro Toyama,[3] Katsunori Yoshinaga,[6] Masayuki Hashimoto,[1] Shuhei Koshizuka,[1] Yutaka Nishio,[1] Chikato Mannoji,[1] Akihiko Okawa[1] and Masashi Yamazaki[1]

Departments of [1]Orthopaedic Surgery, [2]Bioenvironmental Medicine and [3]Anatomy and Developmental Biology, Chiba University Graduate School of Medicine, Chiba, [4]Department of Orthopaedic Surgery, Chiba Aoba Municipal Hospital, Chiba [5]Department of Stem Cell Biology and Histology, Tohoku University Graduate School of Medicine, Sendai, and [6]Chiba Rehabilitation Center, Chiba, Japan

The aim of this study was to evaluate whether transplantation of human bone marrow stromal cell-derived Schwann cells (hBMSC-SC) promotes functional recovery after contusive spinal cord injury of adult rats. Human bone marrow stromal cells (hBMSC) were cultured from bone marrow of adult human patients and induced into Schwann cells (hBMSC-SC) *in vitro*. Schwann cell phenotype was confirmed by immunocytochemistry. Growth factors secreted from hBMSC-SC were detected using cytokine antibody array. Immunosppressed rats were laminectomized and their spinal cords were contused using NYU impactor (10 g, 25 mm). Nine days after injury, a mixture of Matrigel and hBMSC-SC (hBMSC-SC group) was injected into the lesioned site. Five weeks after transplantation, cresyl-violet staining revealed that the area of cystic cavity was smaller in the hBMSC-SC group than that in the control group. Immunohistochemstry revealed that the number of anti-growth-associated protein-43-positive nerve fibers was significantly larger in the hBMSC-SC group than that in the control group. At the same time, the number of tyrosine hydroxylase- or serotonin-positive fibers was significantly larger at the lesion epicenter and caudal level in the hBMSC-SC group than that in the control group. In electron microscopy, formation of peripheral-type myelin was recognized near the lesion epicenter in the hBMSC-SC group. Hind limb function recovered significantly in the hBMSC-SC group compared with the control group. In conclusion, the functions of hBMSC-SC are comparable to original Schwann cells in rat spinal cord injury models, and are thus potentially useful treatments for patients with spinal cord injury.

Key words: axonal regeneration, bone marrow stromal cell, hind limb function, Schwann cell, spinal cord injury.

INTRODUCTION

It has been widely known that central and peripheral nervous systems show quite different reactions when they are injured. The former fails to regenerate, but the latter successfully regenerate their injured axons. The difference in the glial environment may be the key to the discrepancy in regenerating capacity between central and peripheral nervous systems. Oligodendrocytes form CNS myelin which contains inhibitory molecules for axonal regeneration, including myelin-associated glycoprotein, oligodendrocyte myelin glycoprotein and Nogo.[1] In contrast, Schwann cells, which form peripheral myelin, can express various types of neurotrophic factors and adhesion molecules, known to contribute to peripheral nervous system regeneration.[2] Thus, Schwann cells may have the capacity to convert the non-permissive environment for axonal regeneration of the CNS into a permissive one.[3] In fact, many researchers reported that transplantation of

Correspondence: Masao Koda, MD, PhD, Department of Orthopaedic Surgery, Chiba Aoba Municipal Hospital, 1273-2, Aoba-Cho, Chuo-Ku, Chiba 260-0852, Japan. Email: masaomst@yahoo.co.jp

Received 22 January 2010; revised and accepted 30 March 2010; published online 21 June 2010.

Schwann cells can promote axonal regeneration of lesioned adult rat spinal cord.[4]

Recently, we have reported that Schwann cells could be induced from bone marrow stromal cells *in vitro* (bone marrow stromal cell-derived Schwann cell; BMSC-SC) and they effectively promoted regeneration of lesioned sciatic nerves.[5,6] BMSC-SC can also promote axonal regeneration and functional recovery of hind limbs of completely transected[7] and contused[8] adult rat spinal cords, as we have reported previously. As a source of cell transplantation therapy for spinal cord injury, BMSC-SC has some advantages compared with original Schwann cells derived from peripheral nerves. First, BMSC can be easily obtained by bone marrow aspiration.[9] In contrast, harvesting Schwann cells from peripheral nerves needs to scarify the healthy peripheral nerve, resulting in complications including anesthesia or abnormal pain at the harvesting site. Bone marrow aspiration is much less invasive and can be performed in outpatient clinics. Second, BMSC is easily expanded *in vitro* because they can proliferate more vigorously than Schwann cells derived from peripheral nerves.[9] These advantages elevate BMSC-SC to a strong candidate for cell transplantation therapy for spinal cord injury. Recently we reported that human BMSC-SC (hBMSC-SC) can promote regeneration of transected rat sciatic nerves.[10] Thus there is a possibility that hBMSC-SC has a potential to promote hind limb functional recovery after spinal cord injury (SCI) as rat BMSC-SC promoted functional recovery after SCI, as we previously reported.

In the current study, we showed that hBMSC can be induced into Schwann cells characteristics *in vitro* and transplantation of hBMSC-SC reduced cystic cavity, promoted regeneration/sparing of several types of spinal cord axons and accelerated hind limb functional recovery in contusive spinal cord injury in adult rats.

MATERIALS AND METHODS

Human bone marrow stromal cell culture and hBMSC-SC induction *in vitro*

Human bone marrow stromal cells (hBMSC) were collected from a 22-year-old female patient during spinal surgery for benign spinal cord tumor (ependymoma in the conus medullalis region) with informed consent and accordance with the ethical committee of Chiba University Graduate School of Medicine. The cancellous bone in spinous processes was collected, minced and incubated with collagenase D (3 mg/mL, Roche Diagnostics, Basel, Switzerland) 37°C for 1 h to dislodge adherent cells.[11] Then the cells were washed with phosphate-buffered saline (PBS) three times and filtered. The filtered cells obtained from 0.5 mg of the original trabecular bone were plated onto 10-cm plastic dishes. Adherent cells were cultured as hBMSC with alpha-minimum essential Eagle medium (αMEM, Sigma, St Louis, MO, US) supplemented with 20% fetal bovine serum (FBS). Cells grown near confluence were treated with 0.25% trypsin (Sigma) and re-plated onto 10-cm plastic dishes at a split ratio of 1:3. BMSC at passage 1 were subjected to immunocytochemistry, transplantation experiments and Schwann cell induction.

Schwann cell induction was performed as previously described with minor modification.[5,7,10] In brief, hBMSC at passage 1 was incubated with αMEM containing 1 mM beta-mercaptoethanol for 24 h. After washing with PBS, medium was replaced with αMEM containing 10% FBS and 35 ng/mL all-*trans*-retinoic acid (Sigma) for 3 days. Cells were then transferred into αMEM containing 10% FBS, 5 μM forskolin (Calbiochem, La Jolla, CA, US), 10 ng/mL recombinant human basic fibroblast growth factor (Peprotech, London, UK), 5 ng/mL platelet derived-growth factor AB (Peprotech), and 200 ng/mL heregulin (R&D Systems, Minneapolis, MN, US) for 7 days.

To analyze the character of hBMSC and induced hBMSC-SC *in vitro,* we performed immunocytochemistry as previously described.[5,7] Anti-fibronectin (1:400; Chemicon, Temecula, CA, US) and anti-vimentin (1:400; DakoCytomation, Copenhagen, Denmark) were used as markers for marrow stromal cells. Anti-S-100 rabbit polyclonal antibody (S-100, 1:100; DakoCytomation), anti-p75 low affinity nerve growth factor receptor rabbit polyclonal antibody (p75LNGFR, 1:200; Chemicon) and anti-O4 mouse monoclonal antibody (1:400; Chemicon) were used as markers for Schwann cells. Cell nuclei were stained with 4′,6-diamidino-2-phenylindole (DAPI: Molecular Probes, Eugene, OR, US). The negative control was performed by omitting the primary antibodies.

To evaluate cytokines and growth factors secreted from hBMSC and hBMSC-SC, cytokine antibody array analysis was performed. hBMSC and hBMSC-SC were cultured in α-MEM without FBS in 5% CO_2 at 37°C for 24 h and the conditioned media were collected. Cytokines in the conditioned media of hBMSC and hBMSC-SC were investigated using the Human Cytokine Antibody Array® (RayBiotech, Inc., Norcross, GA, US) according to the manufacturer's instructions.

Spinal cord injury and transplantation

Tissue samples were obtained from 25 9-week-old male Wistar rats (average weight 200 g; SLC, Hamamatsu, Japan). Animals were anesthetized with 1.4–1.6% halothane in 1.5 L/min oxygen. Laminectomy was performed at the T9 level, leaving the dura intact. Then the spinal cord was contused with a 10 g weight rod dropped from 25 mm height using an NYU impactor at the T9 level.[12] Muscles

and skin were sutured layer to layer, and the rats placed in warm cages overnight. Manual bladder expression was performed twice a day until recovery of the bladder reflex.

One week after injury, the injured site was re-exposed and transplantation was performed. Mixture of Matrigel (BD Biosciences, Bedford, MA, US) and hBMSC-SC (hBMSC-SC group; 2×10^6 in 5 μL/rat, $n = 9$), Matrigel and hBMSC (hBMSC group; 2×10^6 in 5 μL/rat, $n = 9$) or Matrigel alone (MG group; 5 μL, $n = 7$) was injected into the injured site using a glass micropipette attached with a Hamilton microsyringe. We used Matrigel as a scaffold because Matrigel contains several kinds of extracellular matrices and growth factors and may promote survival of transplanted cells.

After transplantation, the T7 and T10 spinous processes were tied together tightly with a 1-0 silk suture to prevent kyphosis. Food and water were provided *ad libitum*. All the animals were given antibiotics in their drinking water (1.0 mL Bactramin (Roche) in 500 mL acidified water) for 2 weeks after transplantation.

All animals were immunosuppressed with cyclosporine A and dexamethasone. Twenty-four hours before transplantation, cyclosporine A (10 mg/kg) was injected subcutaneously. After transplantation, cyclosporine A was also injected for the entire experimental period (20 mg/kg on Monday and Wednesday, 40 mg/kg on Friday[13]). As an additional immunosuppressant, we used dexamethasone (0.5 mg/kg) 24 h before transplantation, and three times weekly during the first week post-transplantation.

None of the animals showed apparent abnormal behavior during the experimental period. All the experimental procedures were performed in compliance with the guidelines established by the Animal Care and Use Committee of Chiba University.

Tissue preparation

At the end of the functional assessment 6 weeks after injury, animals were perfused transcardially with 4% paraformaldehyde in PBS (pH 7.4) after an overdose of pentobarbital anesthesia. Three spinal cord segments (T8–10) including the injury epicenter were removed and post-fixed in the same fixative overnight, stored in 20% sucrose in PBS at 4°C and embedded in OCT (Sakura Finetechnical, Tokyo, Japan). Sagittal cryosections (20 μm in thickness) were mounted onto poly-L-lysine-coated slides (Matsunami, Tokyo, Japan).

Measurement of cystic cavity

To measure the area of the cystic cavity, every sixth section (120 μm apart) of the central portion of the spinal cords were selected. At least four samples from each animal were picked up, and thus the central 480 μm portion of the lesioned site was evaluated for cystic cavity. The sections were stained with cresyl-violet, dehydrated and sealed with Permount (Fisher Scientific, Fairlawn, NJ, US). We measured the area of the cystic cavity using Scion Image computer analysis software (Scion Corporation, Frederick, MA, US).

Immunohistochemistry

We performed immunohistochemistry as previously described.[7,14] The following primary antibodies were used to detect various types of nerve fibers: anti-growth-associated protein-43 (GAP-43, 1:400; Santa-Cruz Laboratories, Santa-Cruz, CA, US), anti-tyrosine hydroxylase monoclonal antibody (TH, 1:400; Chemicon), anti-serotonin rabbit polyclonal antibody (1:5000; Sigma) and anti-calcitonin gene-related peptide rabbit polyclonal antibody (CGRP, 1:1000; AFFINITI, Exeter, UK). After incubation with primary antibodies, the sections were incubated with Alexa 488-conjugated secondary anitibodies (Molecular Probes) to detect positive signals. We used GAP-43 as a general marker for regenerating/sprouting nerve fibers and the following markers for specific nerve fiber populations. TH-positive nerve fibers are mainly coerulo-spinal adrenergic nerve fibers and serotonin-positive nerve fibers are mainly raphe-spinal serotonergic fibers, both of which contribute to motor function.[15–18] To evaluate regeneration/sparing of GAP-43-, TH- or serotonin-positive nerve fibers, every sixth section was reacted with a specific antibody and the number of immunoreactive fibers that traversed the lines perpendicular to the central axis of the spinal cord at rostral (5 mm rostral to the injury epicenter), epicenter and caudal (5 mm caudal to epicenter) levels were counted in at least four samples from each animal; thus the central 480 μm portion of the graft was evaluated by immunohistochemistry.

To characterize transplanted cells, we performed a double immunofluorescence study for human cell-specific marker and cell-type markers 5 weeks after transplantation in the hBMSC and hBMSC-SC groups. Anti-human mitochondria mouse monoclonal antibody (1:100; Chemicon) was used as a marker for transplanted human-derived cells. Anti-fibronectin and anti-vimentin antibodies were used as markers for marrow stromal cells. Anti-S-100 and anti-p75 antibodies were used as markers for Schwann cells. Anti-microtuble-associated protein 2 antibody (MAP-2, 1:1000; Chemicon) was used as a marker for neurons, GFAP antibody (1:400; Sigma) was used as a marker for astrocytes and anti-myelin basic protein antibody (MBP, 1:200; Chemicon) was used as a marker for oligodendrocytes. After reaction with primary antibodies, sections were incubated with Alexa Fluor 488-conjugated anti-mouse IgG and Alexa Fluor 594-conjugated anti-

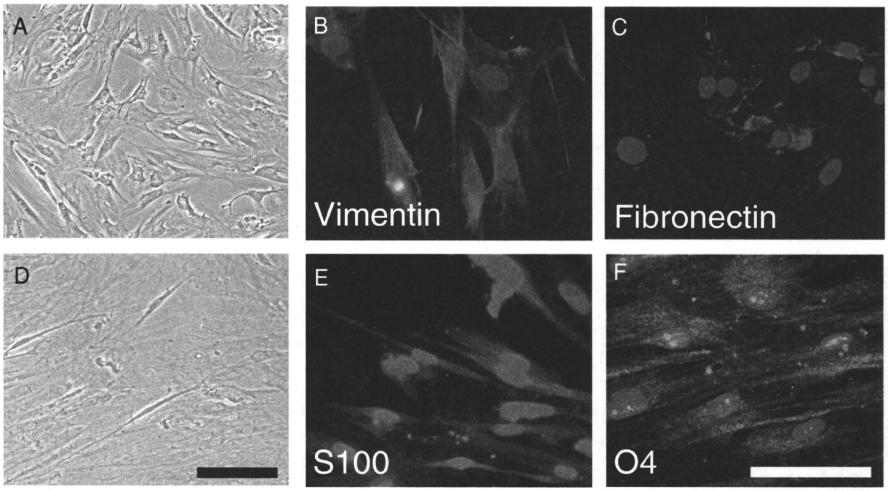

Fig. 1 (A) Phase-contrast microscopic image of human bone marrow stromal cells (hBMSC) cultured from cancellous bone. (B, C) Immunofluorescence of hBMSC for vimentin (B) and fibronectin (C). hBMSC was positive for vimentin and fibronectin. Nuclei were stained with 4′,6-diamidino-2-phenylindole (DAPI). (D) Phase-contrast microscopic image of Schwann cells induced from hBMSC (hBMSC-SC). The hBMSC-SC was morphologically and phenotypically similar to Schwann cells. (E, F) Immunofluorescence image of hBMSC-SC for S-100 (E) and O4 (F). hBMSC-SC was positive to S-100 or O4. Bars = 50 μm.

rabbit IgG (Molecular Probes). The fluorescent signals were observed by fluorescence microscopy (ECLIPSE E600; Nikon, Tokyo, Japan).

Electron microscopy

The rats were perfusion-fixed with 3% glutaraldehyde in HEPES ($C_8H_{18}O_4N_2S$) buffer (10 mM HEPES, 145 mM NaCl) under deep anesthesia. The spinal cord was excised, and part of the spinal cord including the injured site was immersion-fixed for an additional 90 min, after longitudinal slicing. The tissues were then post-fixed with 1% OsO4. After dehydration, the tissues were embedded in Epon. Semi-thin sections (1.5 μm) were stained with toluidine blue and precise areas for electron microscopy were selected and recorded under a light microscope. The semi-thin sections on the slide glass were re-embedded in Epon. Finally, ultra-thin sections from the precise areas were prepared and stained with uranyl acetate and lead citrate for electron microscopy (JEM 1200EX; JEOL, Tokyo, Japan).

Assessment of locomotor activity

Hind limb function of animals in all the groups was assessed using the BBB locomotor scale[19] before injury and 1 day, 3 days, and 1–6 weeks (once a week) after injury.

Statistics

All statistics were evaluated by multiple comparisons between groups. For histological studies, one-way analysis of variance (ANOVA) followed by Bonferroni/Dunn post-hoc test was used. For 6 weeks locomotor scale, repeated-measures ANOVA followed by Fisher's protected least significant difference (PLSD) post-hoc test was used. For fractional BBB score at eight time points, one-way ANOVA followed by Bonferroni/Dunn test was used. Differences were accepted for statistical significance at $P < 0.05$* and $P < 0.01$**.

RESULTS

Induced hBMSC-SC was apparently different in their morphology from that of original hBMSC. hBMSC showed fibroblast-like morphology but after induction they changed into spindle-shaped morphology similar to the Schwann cells (Fig. 1A,D). Immunocytochemistry showed that hBMSC was positive for fibronectin and vimentin (Fig. 1B,C) and induced hBMSC-SC was positive for S-100, O4 (Fig. 1E,F) and P75LNTFR (not shown), widely-known markers for Schwann cells. The percentage of cells positive for S-100, O4 and p75LNTFR after Schwann cell induction

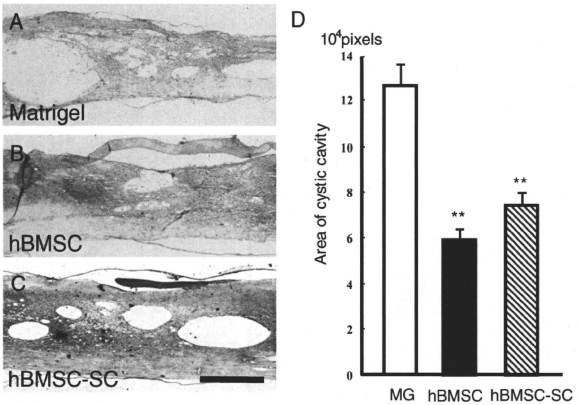

Fig. 2 Measurement of cystic cavity. The sections were stained with cresyl-violet. We measured the area of the cystic cavity using Scion Image computer analysis software. Arrows indicate the cystic cavity in the lesioned spinal cord. (A) In the Matrigel alone (MG) group, large cystic cavity formation was observed. (B, C) In the human bone marrow stromal cells (hBMSC) and Schwann cells induced from hBMSC (hBMSC-SC) groups, the area of cystic cavity was smaller than that of the MG group. (D) Statistical analysis of area of cystic cavity. In the hBMSC (closed column) and hBMSC-SC (hatched column) groups, the area of cystic cavity was significantly smaller than that of the MG group (open column). $*P < 0.01$. Bar = 1 mm in (A–C) and bars = ± SE in (D).

in vitro were all approximately 95%. Thus induced hBMSC-SC is morphologically and phenotypically identical to Schwann cells, as we described previously in rat BMSC.[7]

Next we performed cytokine assay using antibody array. The following factors were detected in hBMSC-SC-conditioned media: macrophage chemoattractant protein-1 (MCP-1), interleukin-6 (IL-6), insulin-like growth factor binding protein 2 and 4 (IGFBP-2 and 4), tissue inhibitor of metalloproteinase-1 and 2 (TIMP1 and 2) vascular endotherial growth factor (VEGF), urokinase receptor (uPAR), soluble tumor necrosis factor alpha receptor-1 (sTNF-αR) and interleukin-8 (IL-8) (Supporting Fig. S1).

Five weeks after transplantation, we measured the area of cystic cavity with cresyl violet staining (Fig. 2A–C). In the hBMSC (Fig. 2B,D, closed column) and hBMSC-SC (Fig. 2C,D, hatched column) groups, the average area of cystic cavity was significantly smaller than that in the MG group ($P < 0.01$; Fig. 2A,D, open column), indicating that transplantation of hBMSC or hBMSC-SC preserved spinal cord tissue. There was no significant difference between the hBMSC and hBMSC-SC groups in the cystic cavity area (Fig. 2D).

Next, we performed immunohistochemistry to evaluate axonal regeneration/sparing. The present results revealed that the number of GAP-43-positive nerve fibers at all three levels in the hBMSC-SC group was significantly larger than those in the MG and hBMSC groups ($P < 0.01$) (Figs 3A–C,4A). There was no significant difference between the MG and hBMSC groups in the number of GAP-43-positive nerve fibers at all three levels of the spinal cord (Fig. 4A).

To characterize the phenotype of regenerating/spared axons, we performed immunohistochemistry for nerve fiber markers. The numbers of TH-positive nerve fibers at the epicenter and caudal levels in the BMSC and hBMSC-SC groups were significantly larger than those in the MG group ($P < 0.01$) (Figs 3D–F, 4B). Furthermore, the number of TH-positive nerve fibers in the hBMSC-SC group was larger than that in the hBMSC group ($P < 0.05$; Fig. 4B). The number of serotonin-positive nerve fibers in the hBMSC and hBMSC-SC groups was apparently larger than that in the MG group at the epicenter and caudal levels ($P < 0.01$; Figs 3G–I, 4C). At the epicenter, the number of serotonin-positive nerve fibers was not statistically different between the hBMSC and hBMSC-SC groups. At the caudal level, the number of serotonin-positive fibers in the hBMSC-SC group was significantly larger than that in the hBMSC group ($P < 0.05$; Fig. 4C).

Double immunofluorescence study showed that almost all of human mitchondria-positive transplanted hBMSC were simultaneously positive for fibronectin or vimentin (not shown) and that all hBMSC-SC were also positive for S-100 (Fig. 5A–C, arrowhead) or p75LNGFR (not shown). The percentage of those indicating that transplanted hBMSC and hBMSC-SC maintained their specific phenotype observed *in vitro* even after transplantation. In addition, S100- or p75LNGFR-positive cells without human mitchondria immunoreactivity were observed around the lesioned site of the spinal cord (Fig. 5A–C), suggesting that endogenous Schwann cells migrated into the lesioned site. Those endogenous Schwann cells were also observed in the MG and hBMSC groups. There was no statistical difference in the number of endogenous Schwann cells between the groups (not shown). The number of human mitochondria-

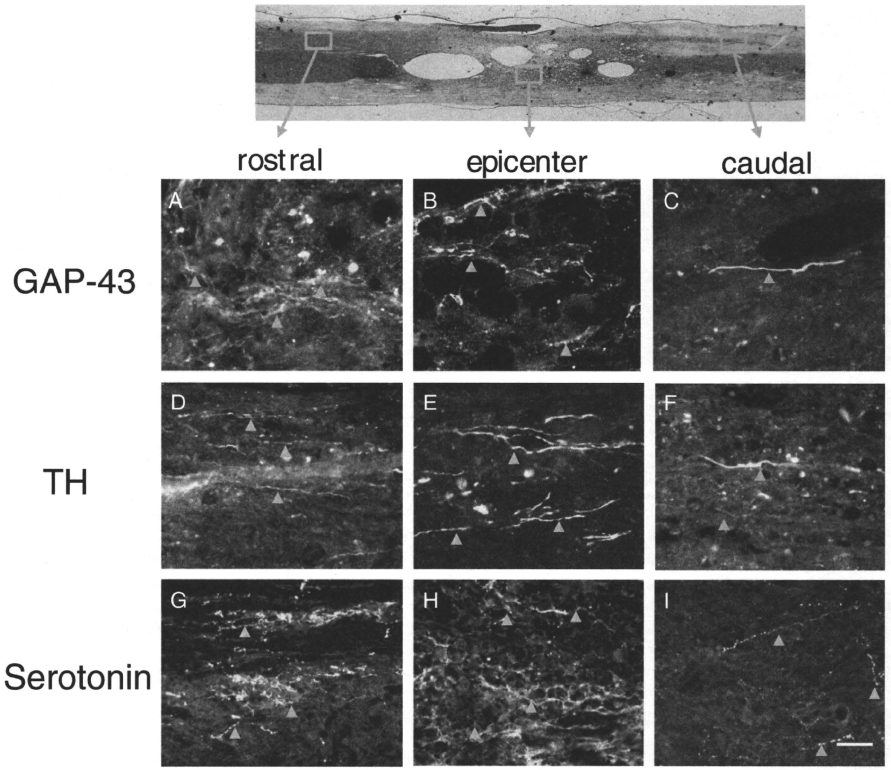

Fig. 3 Immunohistochemistry for nerve fiber markers in the Schwann cells induced from human bone marrow stromal cells (hBMSC-SC) group. Anti-growth-associated protein-43 (GAP-43)-positive fibers (A–C, arrowheads), tyrosine hydroxylase (TH) -positive fibers (D–F, arrowheads) and serotonin-positive fibers (G–I, arrowheads) were detected at the rostral, epicenter and caudal levels. Bar = 50 μm.

positive cells in the hBMSC and hBMSC-SC groups was 9.5 ± 2.0 and 10.2 ± 2.2 per section, respectively (not shown). There was no statistical difference in the number of human mitochondria-positive cells between the two groups. We could not detect cells that were double positive for human mitochondria and neural lineage markers (not shown).

In electron microscopic study of the hBMSC-SC group, myelin with basement membrane which is a specific feature of peripheral-type myelin formed by Schwann cells was observed near the lesioned site (Fig. 6A,B).

Finally, we assessed the recovery of hind limb function in all the three groups (Fig. 7). Hind limb function significantly recovered in both the hBMSC-SC ($P < 0.01$, Fig. 7, circle) and hBMSC ($P < 0.05$, Fig. 7, triangle) groups compared with the MG group (Fig. 7, square) from 4 weeks after transplantation, and a significant difference from the MG group was recognized up to 5 weeks after transplantation. The average recovery score in the hBMSC-SC group 5 weeks after transplantation was 11.7 ± 0.8, which indicates frequent to consistent weight-supported plantar steps and occasional fore limb–hind limb coordination, and recovery score in the hBMSC group was 10.5 ± 1.5, which indicates occasional weight-supported plantar steps without fore limb–hind limb coordination. There was no significant statistical difference between the hBMSC-SC

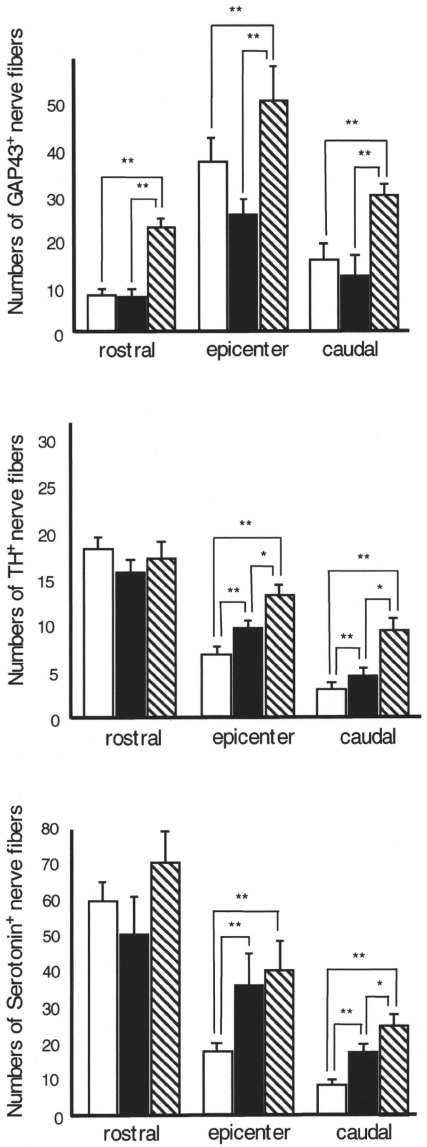

Fig. 4 Comparison of the average number of GAP-43-, tyrosine hydroxylase (TH)- and serotonin-positive fibers among the groups. Immunohistochemistry for anti-growth-associated protein-43 (GAP-43), TH and serotonin were performed and the number of immunoreactive fibers that traversed the lines perpendicular to the central axis of the spinal cord at rostral (5 mm rostral to the injury epicenter), epicenter and caudal (5 mm caudal to epicenter) levels were counted. The numbers of GAP-43-positive fibers were significantly larger in the Schwann cells induced from human bone marrow stromal cells (hBMSC-SC) group (A, hatched column) than those in the Matrigel alone (MG) (A, open column) and hBMSC (A, closed column) group at all three levels (**$P < 0.01$). The numbers of TH-positive fibers were significantly larger in the hBMSC (B, closed column) and hBMSC-SC (B, hatched column) groups than that in the MG group (B, open column) at the epicenter and caudal levels (**$P < 0.01$). Further, the numbers of TH-positive fibers in the hBMSC-SC group rats at the epicenter and caudal levels were significantly larger than that of the hBMSC group rats (*$P < 0.05$). The numbers of serotonin-positive fibers of the hBMSC (C, closed column) and hBMSC-SC (C, hatched column) groups were significantly larger than that of the MG group (open column) at the epicenter and caudal levels (**$P < 0.01$). There was no significant difference between the hBMSC and hBMSC-SC groups in the number of serotonin-positive fibers at all three levels. Closed columns: MG group; Open columns: BMSC-SC group. Bars = ± SE.

group and the hBMSC group in average BBB score at any time points. In the MG group, the average recovery score 5 weeks after transplantation was 7.67 ± 1.0, which indicates all three joints of hind limbs had extensive movement.

DISCUSSION

In the present study, transplantation of both hBMSC and hBMSC-SC reduced the cystic cavity and promoted modest axonal regeneration/sparing, which resulted in the recovery of hind limb function after contusive injury of the adult rat spinal cord. Transplantation of hBMSC-SC showed stronger axonal regeneration/sparing-promoting effect compared with hBMSC. We have already reported that BMSC-SC can promote axonal regeneration and functional recovery in a complete transaction model of adult rat spinal cord. For future clinical application, we need to prove the efficacy of the treatment for compression- or contusion-induced spinal cord injury, both of which are more relevant to clinical spinal cord injury than transection or hemisection models.[20] Thus we employed a contusive injury model using an NYU impactor, which is one of the gold standard models to study spinal cord injury treatment, and could successfully prove the efficacy of hBMSC-SC transplantation for that model.

Possible explanations of functional recovery obtained by transplantation of hBMSC-SC are as follows. First, hBMSC-SC has neuroprotective effects. Correlation